A New Subcloud Model for Mass-Flux Convection Schemes: Influence on Triggering, Updraft Properties, and Model Climate

CHRISTIAN JAKOB*

ECMWF, Reading, United Kingdom

A. PIER SIEBESMA

KNMI, De Bilt, Netherlands

(Manuscript received 6 September 2002, in final form 5 May 2003)

ABSTRACT

All convection parameterizations in models of the atmosphere include a decision tree to decide on at least the occurrence, and often the type, of convection in a model grid volume. This decision tree is sometimes referred to as the ''trigger function.'' This study investigates the role that the decision-making processes play in the simulation of convection in the European Centre for Medium-Range Weather Forecasts global forecast model.

For this purpose, a new simple parcel-ascent model based on an entraining plume model is developed to replace the currently used undilute ascent in the initial decision making. The consequences of the use of the more realistic model for the behavior of convection itself and its impact on the model climate are investigated. It is shown that there are profound changes to both the convection characteristics, and consequently, the model climate. The wider implications of the findings here for the general design of a mass-flux convection parameterization are discussed.

1. Introduction

One of the most difficult and yet important processes to be described in a general circulation model (GCM) of the atmosphere is that of moist convection. The difficulties arise to a large extent from the subgrid nature of the processes involved in moist convection, requiring their treatment in a GCM by means of parameterization. The situation is not helped by our limited understanding of convection and its interaction with the circulation systems it is embedded in. Despite significant progress, as reflected in the large number of parameterization schemes in use today (e.g., Arakawa and Schubert 1974; Tiedtke 1989; Gregory and Rowntree 1990; Randall and Pan 1993; Hack 1994; Zhang and McFarlane 1995; Emanuel and Zivkovic-Rothman 1999; Donner et al. 2001), it is probably fair to state that up to this day the convection parameterization problem remains unsolved.

A hierarchy of decision-making processes needs to be employed for every convection scheme. The best-known and widely discussed is that of the presence of convection at a model grid point, often referred to as the ''trigger function'' (e.g., Kain and Fritsch 1992). Other, less discussed examples include a decision on the location of the maximum cloud top and the definition of cloud-base properties as required in mass-flux convection schemes. It is the purpose of this paper to investigate the importance of the decision-making algorithm employed in the convection scheme of the operational model of the European Centre for Medium-Range Weather Forecasts (ECMWF) and to derive conclusions for the design of mass-flux convection parameterizations in general.

The ECMWF convection parameterization follows the bulk mass-flux approach and is described in Tiedtke (1989) and Gregory et al. (2000). In the scheme, three major decisions are made before the actual solution of the parameterization equations:

- A decision on the occurrence of convection at a given grid point (i.e., the triggering)
- A decision on the cloud top and therefore the type of surface-driven convection (two types—namely, deep and shallow convection—are distinguished)
- The determination of the location of cloud base and the bulk updraft properties at cloud base (i.e., the closure)

All three decisions are made based on a simple undilute

* Current affiliation: BMRC, Melbourne, Victoria, Australia.

Corresponding author address: Christian Jakob, BMRC, GPO Box 1289K, Melbourne, VIC 3001, Australia.
E-mail: c.jakob@bom.gov.au

parcel ascent of a near-surface air parcel and are essentially based on assessing the parcel buoyancy at the model's discrete levels. Although computationally cheap, this approach to describing a parcel ascent is not physically realistic. It is increasing the physical realism that provides our main motivation for this study. We attempt to achieve this aim by developing a new decision-making algorithm. Its basis is a strong updraft model for the convective subcloud layer developed by Siebesma and Teixeira (2000), which we extend to the cloud layer to replace the simple undilute parcel model. The key parameter used for decision making in the new algorithm is the updraft vertical velocity. It is worthwhile noting at this point that introducing more physical realism into a model does not automatically lead to improved simulations, usually because of shortcomings in other model components. Therefore we do not a priori expect improvements in the overall model behavior but rather aim to investigate in what way the trade-off between realism and computational expense affects the overall model simulations, independent of the direction of model response.

The new algorithm, together with the currently used method, is described in section 2. The direct influence of the new algorithm on the model convection, as well as sensitivities to parameter choices, is investigated using single time step experiments. The experiment setup and results are discussed in section 3. After examining the influence of the new algorithm in the single time step integrations, we study its effect on the convection later in the simulation. This is followed by investigations of the effects the new algorithm has on the model climate. The results are presented in section 4. We close with a brief discussion and some conclusions for the future design of trigger function algorithms for GCMs.

2. The parcel model

Traditionally, a convection scheme parameterizes vertical turbulent transport within the cloud layer. As a precursor, several preliminary steps are required. First, a decision needs to be made whether convection takes place or not. This process is often referred to as the trigger function. Furthermore, if different types of convection are possible (deep/shallow), a decision-making process for their occurrence needs to be defined as well. Last, there is a boundary condition issue: the convection scheme needs to be supplied with the cloud-base height z_b and updraft values at this height of the mass flux M_b, vertical velocity w_u, specific humidity $q_{v,u}$, and temperature T_u. This is usually achieved by employing a subcloud scheme. In this section we will first describe how these processes are parameterized in the current ECMWF scheme. Subsequently, we will introduce and motivate a new formulation that is based on a recently developed new boundary layer scheme.

a. Present formulation of the ECMWF model

At present, the existence of convection is tested by an undiluted ascent of a parcel that is initialized at the lowest model level in the surface layer, with the temperature and humidity at that level. If this undiluted parcel finds a cloud base—that is, the lowest level where it becomes supersaturated—with a parcel buoyancy larger than -0.5 K everywhere between the surface and the cloud-base level, then convection is initiated. This choice is simply related to the assumption that a rising parcel has enough kinetic energy to penetrate through subcloud levels despite a negative buoyancy down to -0.5 K. Subsequently, an initial guess of cloud-top height is made by extending the undilute ascent of the parcel, including condensation effects, until it finds its zero buoyancy level. The level where this occurs is used as the first guess for cloud-top height. The distinction between deep and shallow convection is based on the cloud depth, that is, the difference between this initial guess of cloud-top height and cloud-base height. If the cloud depth exceeds 200 hPa, deep convection is assumed, otherwise shallow convection.

The same undiluted ascent is also used to obtain cloud-base values for temperature and humidity. Since no vertical momentum equation is used in the subcloud layer, the in-cloud vertical velocity at cloud base is arbitrarily set to 1 m s^{-1}. Finally, the cloud-base mass flux M_b is determined. In the case of deep convection, M_b is dictated from the assumption that the convection reduces the convective available potential energy (CAPE) toward zero over a specified timescale τ (Fritsch and Chappell 1980; Gregory et al. 2000). This relaxation time τ is typically of the order of 1 h, but its precise value is made dependent on the horizontal model resolution. In the case of shallow convection, this CAPE closure is not used. Instead, a boundary layer equilibrium closure is used: the cloud-base mass flux M_b is chosen so as to sustain a neutral budget for the moist static energy h in the subcloud layer:

$$M_b(h_{u,b} - \overline{h}) = -\int_0^{z_b} \left[\overline{\mathbf{v}} \cdot \nabla \overline{h} + \overline{w} \frac{\partial \overline{h}}{\partial z} + c_p \left(\frac{\partial \overline{T}}{\partial t} \right)_{\text{rad}} + \frac{1}{\overline{\rho}} \frac{\partial}{\partial z} (\overline{\rho} \overline{w'h'})_{\text{turb}} \right] \overline{\rho}\, dz. \quad (1)$$

The right-hand side of (1) contains the sources and sinks of h due to large-scale advection, subsidence, radiative cooling or heating, and turbulent fluxes of the boundary layer scheme. Usually, the dominant contribution originates from the surface flux, in which case this closure reduces to

$$M_b(h_{u,b} - \overline{h}) = \overline{w'h'}_{\text{srf}}. \quad (2)$$

b. A new parcel model

A new model for strong updrafts in the convective boundary layer has recently been developed for use in

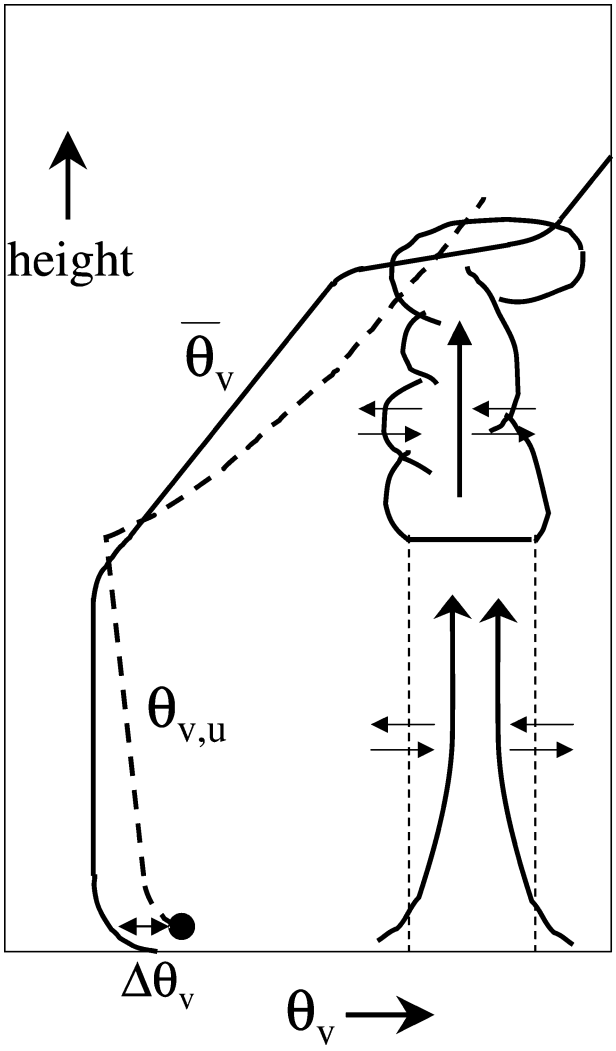

FIG. 1. A schematic of the new parcel model. Note that in comparison to the current model updraft vertical velocity rather than parcel buoyancy is the key parameter in the decision making.

the ECMWF parameterization package (Siebesma and Teixeira 2000). Its motivation grew out of the increasing need to have a more coherent parameterization of turbulent transport in the clear and cloudy boundary layers. To this purpose, one single formulation for strong updrafts that can be used in both the clear and cloudy boundary layers has been formulated (Fig. 1). The ultimate objective is to parameterize the transport associated with these strong updrafts (in both clear and cloudy conditions) with one single mass-flux scheme, whereas the transport due to the remaining smaller eddies can be parameterized by a more local diffusive approach. However, in this study we use this new updraft model only as a more physical update for the presently used undiluted parcel ascent described in section 2a.

A proper definition of strong updrafts that is valid in both the cloud layer and in the subcloud layer is not without problems. The widely used cloud core definition (Siebesma and Cuijpers 1995)—that is, updrafts that are positively buoyant and within clouds—obviously can not be used in the subcloud layer and the dry boundary layer. Therefore we define strong updrafts as those areas that contain the highest positive vertical velocities. More precisely, in the large eddy simulation (LES) analysis that has been used to design and evaluate this parameterization (van Ulden and Siebesma 1997; Siebesma and Teixeira 2000), strong updrafts are simply defined as a fraction a_u of all the grid points on a horizontal slab that contain the highest vertical velocities. By choosing a value of $a_u \simeq 0.03$, it has been checked that this definition coincides with the cloud core definition near cloud base so that a continuous formulation between the cloud layer and subcloud layer is guaranteed.

The model that has been proposed for the strong updrafts is a simple entraining plume model (Siebesma and Teixeira 2000). It is most conveniently defined in terms of moist conserved variables, such as the moist static energy $h = c_p T + gz + Lq_v$ and the total specific humidity $q_t = q_v + q_l$ (Betts 1973). It is worthwhile noting that there are limitations to the description of convection using the entraining plume assumption. Several authors (e.g., Raymond and Blyth 1986) have shown that observations of cumulus convection can be matched more closely when applying a multiple parcel ascent. However, since the main part of the convection scheme used here is based on an entraining plume model, it is appropriate to base our extension to the decision-making model on the same assumption.

A generic equation for the evolution with height of a conserved updraft property ϕ_u can be written as

$$\frac{\partial \phi_u}{\partial z} = -\varepsilon(\phi_u - \overline{\phi}) \quad \text{with } \phi = \{h, q_t\}, \tag{3}$$

where ε is the fractional entrainment rate. Assuming no subgrid variability within the updraft, a simple additional calculation of the saturation specific humidity $q_s(p, T)$ allows a determination of specific humidity q_v, cloud liquid water/ice content q_l, and temperature T. A simple ''microphysics'' parameterization is added to the updraft equations by removing any condensate in excess of 0.5 g kg^{-1}. The water-loading effect of the remaining condensate is taken into account in the parcel buoyancy calculations. The effects of freezing are taken into account through a gradual transition from water to ice in the temperature range 273.16–250.16 K.

The fractional entrainment rate has been the subject of many recent studies (Siebesma and Cuijpers 1995; Grant and Brown 1999; Gregory 2001; Neggers et al. 2002). LES studies of the convective boundary layer indicate that the fractional entrainment rate behaves in the lower part of the boundary layer as (van Ulden and Siebesma 1997; Siebesma and Teixeira 2000; de Roode et al. 2000)

$$\varepsilon \simeq c_e \frac{1}{z} \quad \text{with } c_e \simeq 0.55. \tag{4}$$

For shallow cumulus convection, typical values of $\varepsilon \simeq 1 \sim 3 \times 10^{-3}$ m^{-1} are reported, both from LES studies (Siebesma and Cuijpers 1995) and observational studies (Raga et al. 1990). For deep convection, cloud-resolving models (CRMs) suggest values of ε of the order of 10^{-4} m^{-1}. Here (4) is used as a parameterization in the simple updraft model (3); it has the correct behavior in the lower part of the subcloud layer, and it interpolates smoothly to typical values found for shallow and deep convection. Moreover, simple scaling arguments in the cloud layer also support (4) (Siebesma 1998).

The updraft model is initialized by taking the mean value at the lowest model level z_1 and adding an excess that scales with the surface flux (Troen and Mahrt 1986):

$$\phi_u(z_1) = \overline{\phi}(z_1) + b\frac{\overline{w'\phi'}_s}{\sigma_w(z_1)}, \tag{5}$$

where $\overline{w'\phi'_s}$ is the surface flux. The value of the prefactor $b \simeq 1$ is based on LES results (Siebesma and Teixeira 2000). For the standard deviation σ_w near the surface, we use an empirical expression based on a combination of atmospheric data, tank measurements, and LES data (Holtslag and Moeng 1991):

$$\frac{\sigma_w}{w_*} \simeq 1.2\left[\left(\frac{u_*}{w_*}\right)^3 + 0.6\frac{z}{z_i}\right]^{1/3}, \tag{6}$$

where w_* is the usual convective velocity scale, and u_* is the friction velocity.

In addition, an equation for the vertical velocity (Simpson and Wiggert 1969) is employed:

$$w_u\frac{\partial w_u}{\partial z} = -c_1\varepsilon w_u^2 + c_2 B \quad \text{with } w_u(z_1) = \sigma_w, \tag{7}$$

with a buoyancy term $B = g(\theta_{v,u} - \overline{\theta_v})/\overline{\theta_v}$ as an extra source term. The coefficients c_1 and c_2 take into account the pressure perturbations and subplume turbulence terms. The same values, $c_1 = 2$ and $c_2 = 1/3$, that are currently already used in the full convection parameterization are adopted for the first-guess ascent. These values are varied to study the sensitivity of this choice.

Finally, the definition of the discrete cloud-base level is also altered. In the original formulation this was the lowest model level where the rising parcel is supersaturated. In the new formulation the exact cloud-base pressure is calculated. The discrete model level closest to this pressure is then defined to be the discrete cloud-base level. This way a systematic overestimation of cloud-base height is removed.

The new formulation of the first-guess parcel ascent has a number of advantages over the previous one. First, the overly simple dependence on buoyancy together with an artificial threshold in virtual temperature excess of -0.5 K, as used in the previous trigger function, becomes obsolete. Such a simple trigger function assumes that a parcel always has the same amount of kinetic energy that is just enough to overcome a potential barrier near cloud base of -0.5 K. In the present situation the amount of kinetic energy gained by the rising parcel in the subcloud layer is explicitly calculated by the vertical velocity equation (7). If cloud base is found while the vertical velocity is still positive, cumulus convection is initiated. The new preliminary cloud-top height is now simply defined as the height at which the updraft vertical velocity vanishes. This way the overshoot of convective clouds into an inversion is taken into account. Second, the present form of the entrainment rate of the updraft model has the advantage that the precise choice of the initialization height z_1 becomes less relevant. More precisely, if $\overline{\phi}$ has a logarithmic profile, as is common in the surface layer, one can show that for $\varepsilon \sim 1/z$, the excess $\phi_u - \overline{\phi}$ becomes height independent. As a result, the only height dependence is in the excess formulation (5).

3. Single time step experiments

a. Motivation and experiment setup

Before introducing a new parameterization into the full GCM and assessing its impact on either forecast performance or model climate, it is desirable to understand its workings in a more simplified setup. The most commonly used of such setups is the so-called single-column model (SCM) (e.g., Randall et al. 1996). A single column of the GCM is extracted and, by prescribing the large-scale conditions normally predicted in the full GCM, the response of the physical parameterizations to that forcing can be studied easily in detail. Although this approach is computationally cheap and in widespread use, one of its major drawbacks is the scarcity of suitable case prescriptions currently available.

Here a different approach is followed. The direct impact of the new algorithm described in section 2 is examined by performing a single time step integration of the full GCM rather than relying on SCM simulations. That way the parameterizations that are the subjects of the comparison are exposed to a large number of identical atmospheric conditions, and their response can be studied without allowing for feedback. This provides a first indication of how the introduction of any new parameterization will directly affect the model. This method was successfully applied before by Jakob and Klein (1999, 2000) when investigating the impact of a parameterization of cloud fraction effects on microphysics.

It is obvious that this method is not sufficient for understanding what impact a changed parameterization has on the full GCM. However, it will provide crucial information on the detailed working of the scheme, which will assist in the interpretation of the results of longer model integrations in which complex feedback processes will have occurred.

In order to facilitate the comparison, the ECMWF model was integrated using various versions of the first-guess parcel treatment for one time step at a horizontal resolution of T_L95, with 60 model levels in the vertical.

TABLE 1. Model versions used in this study.

Acronym	Model description
CTRL	Control model (ECMWF model cycle CY23R3)
NCUB	Same as CTRL, but with the new cloud-base algorithm, as described in section 2
EPS2	Same as NCUB, but with $\varepsilon = 2\ c_\varepsilon/z$
EPSH	Same as NCUB, but with $\varepsilon = 0.5\ c_\varepsilon/z$
EPS0	Same as NCUB, but with $\varepsilon = 0$
W1	Same as NCUB, but with $c_1 = 1$ and $c_2 = 1$ in Eq. (7)
W1P5	Same as NCUB, but with $c_1 = 1$ and $c_2 = 1.5$ in Eq. (7)
CLEV	Same as NCUB, but with cloud base always at top half-level (see section 2)

A description of the different model versions can be found in Table 1. The initial conditions for all experiments were arbitrarily chosen to be those of 1 May 1987 and are taken from ECMWF's reanalysis (Gibson et al. 1997) archive. The results are analyzed on the model's native reduced linear grid (Hortal 1999) to avoid any influence of interpolation between grid points.

b. Results

As described in section 2, the decision-making algorithms under investigation provide the following information to the convection scheme: the existence of surface-driven convection, an initial estimate of convective cloud depth on which the decision on the type of convection is based, and the updraft properties at cloud base. In this section these quantities will be analyzed in the single–time step experiments for the various model versions in Table 1.

The most basic decision that the decision-making algorithms need to provide is that of the existence of surface-driven convection at a given model grid point. Furthermore, an initial estimate of the expected cloud depth is used in both algorithms to determine the prevalent type of convection, that is, deep or shallow. Figure 2 shows the relative frequency of occurrence of surface-driven convection separated into the deep and shallow types allowed for by the parameterization. The results are taken from the tropical and subtropical belt only (30°N–30°S, approximately 6000 model grid points). This area will be loosely referred to as the Tropics hereafter.

The parameterization using the new algorithm produces significantly less grid points with convection than the current one. The total fraction of points with convection is reduced from 0.74 in CTRL to 0.5 in NCUB. The ratio of deep to shallow convective points in CTRL is 0.32; it reduces to 0.27 in NCUB, indicating a relatively stronger influence of the new algorithm on deep convection. The various sensitivity experiments lead to variations in both the number of deep and shallow points. However, all of the experiments yield significantly less points with shallow convection. Further in-

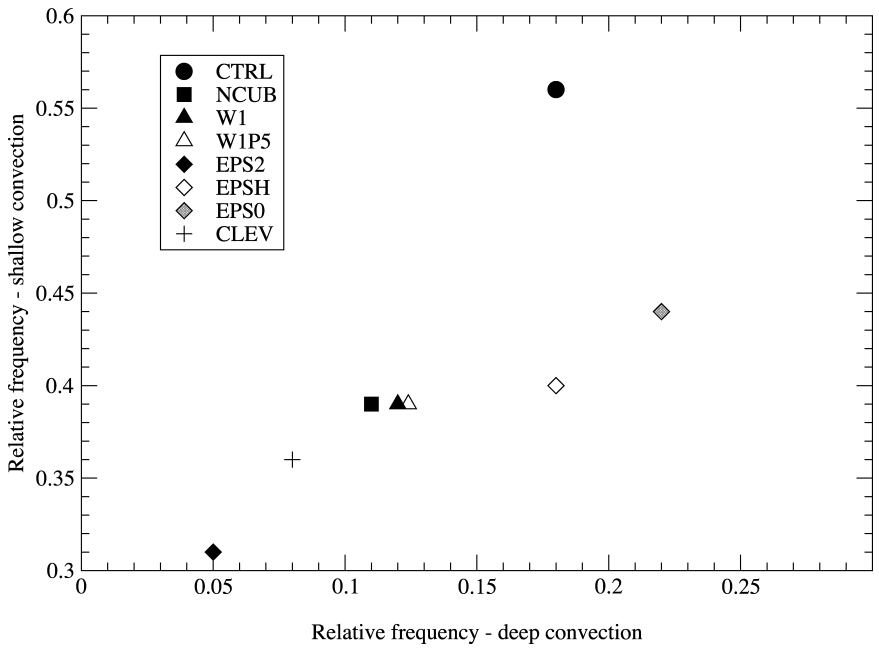

FIG. 2. Occurrence of surface-driven convection for the various model versions. Results are from the first time step of a T95L60 forecast and for the latitude band 30°N–30°S.

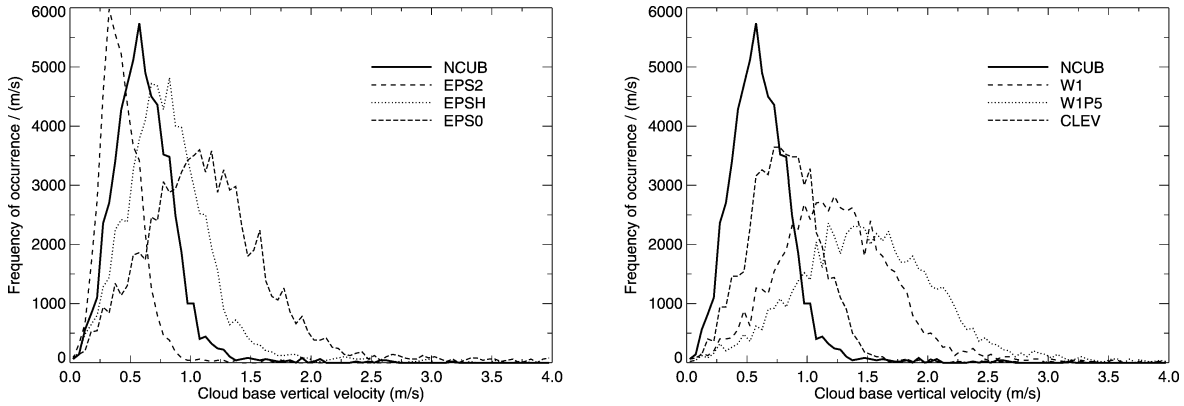

FIG. 3. Frequency distribution of updraft vertical velocity at cloud base. Results are from the first time step of a T95L60 forecast and for the latitude band 30°N–30°S. The frequency of occurrence has been normalized per unit vertical velocity.

vestigation reveals that the largest drop in convection occurs because the vertical velocity equation at many points yields negative w_u well before cloud base is reached. The current algorithm allows points with negative T_v-excess up to -0.5 K to still be classified as convective, while in the new algorithm negative excess will quickly lead to vanishing w_u, and hence the updraft will terminate.

There is a large sensitivity to the choice of entrainment coefficient. The smaller the entrainment, the larger the number of convective points as expected. None of the entrainment coefficients, however, yields as much convection as the current algorithm, not even the undiluted ascent. This indicates the importance of other parts of the NCUB algorithm. Although for deep convection low entrainment leads to similar or even larger occurrences compared to CTRL, the occurrence of shallow convection remains significantly lower throughout. As outlined above, this is mainly because of the use of the vertical velocity instead of parcel buoyancy for the decision making. Perhaps surprisingly, the results are not very sensitive to the choice of coefficients in the vertical velocity equation, indicating some robustness in the use of this parameter for the decision making.

Changing the algorithm for choosing the location of the discrete cloud-base level also has a nonnegligible effect on the number of convective points. It is remarkable that this effect is larger than that of the choice of vertical velocity equation coefficients. Further investigation reveals that the change in convection occurrence, as seen in Fig. 2, is caused by two separate effects. First and foremost, a significant number of points (351 out of 2380) that have shallow convection in NCUB have no convection at all in CLEV. This can be understood as a result of poor vertical discretization. Clouds that are single-layer clouds in NCUB—that is, those for which the vertical velocity drops to zero immediately above cloud base—will be assigned as ''nonconvective'' in CLEV, since the cloud-base level here coincides with the first layer where the vertical velocity is zero. The drop in occurrence of shallow convection is partly compensated for by a shift from deep to shallow convection (127 out of 649 points).

Now that the occurrence of convection has been determined, some of the updraft properties at cloud base will be compared. First, the frequency distribution of updraft vertical velocity is shown in Fig. 3. Note that CTRL is absent in these figure panels since its first-guess algorithm does not evaluate the vertical velocity. The distributions of all experiments peak well away from zero w_u. This indicates that the points that were deemed nonconvective have been filtered out well before reaching cloud base. NCUB provides a distribution with a peak around $+0.6$ m s^{-1}. The sensitivity to the choice of coefficients is as expected. Larger c_2 and smaller c_1 lead to higher values of w_u. Since the entrainment rate enters the vertical velocity equation, it is not surprising to see a large sensitivity to the choice of ε. The choice of the discrete cloud-base level to be always the top level of the first level with condensation leads to a shift toward higher w_u. This can be understood by realizing that (i) as shown above, this choice leads to less convective points where the weaker updrafts have been filtered out and (ii) the lower part of the convective updrafts is usually marked by acceleration.

Because of its strong relation to parcel buoyancy, another crucial cloud-base parameter to investigate is the virtual temperature excess. This excess has a direct influence on CAPE and is strongly related to the moist static energy excess, both of which are important ingredients of the closure assumptions used in the parameterization. Figure 4 shows the frequency distribution of this variable for the Tropics. There is a large difference between the CTRL and the NCUB models. While CTRL shows a broad distribution of T_v excess peaking around 0.3 K, NCUB exhibits a much narrower distribution, with its peak just above zero. Both models have a number of cases with negative values, with an explicit cutoff at -0.5 K in CTRL. At first thought, one would ascribe the differences in the distributions to the fact that NCUB is a strongly entraining plume, while the updraft in CTRL is undiluted. However, the sensitivity

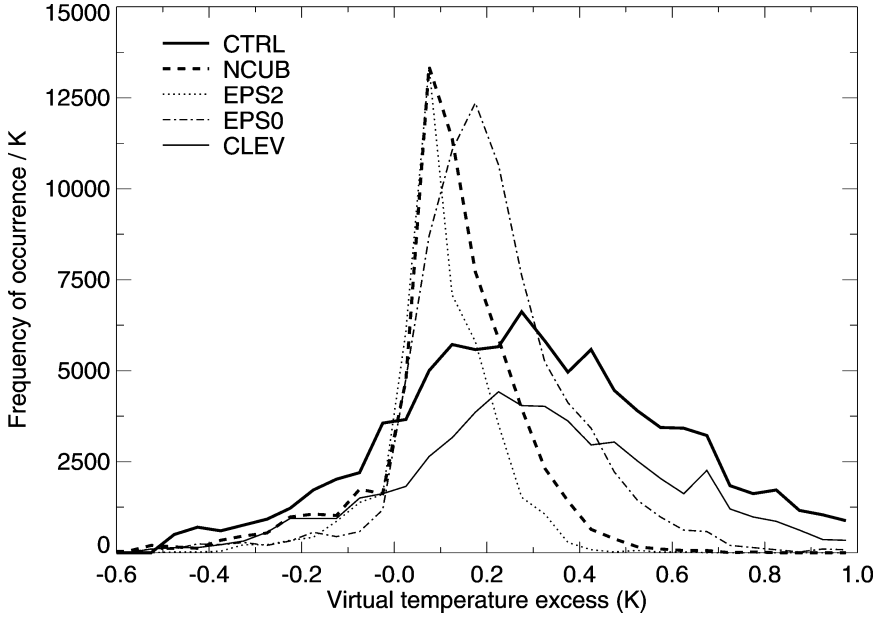

FIG. 4. Frequency distribution of virtual temperature excess at cloud base. Results are from the first time step of a T95L60 forecast and for the latitude band 30°N–30°S. The frequency of occurrence has been normalized per unit temperature.

to entrainment rate shown in Fig. 4 suggests that although lower entrainment leads to higher excess values on average, the shape of the distribution does not change significantly. Changes to the vertical velocity equation show an even smaller sensitivity, and the results are therefore omitted from the figure. Interestingly, it is the CLEV model that leads to a similar distribution shape as found in the CTRL model, indicating that the choice of the discrete level for cloud base plays a significant role in determining the shape of distribution.

This can be understood by considering the evolution of the virtual potential temperature, θ_v, during a parcel ascent together with an environmental profile. In the subcloud layer the virtual temperature of the parcel, $\theta_{v,u}$, is conserved and higher than that of the environment. In a typical convective environment, the subcloud layer is well-mixed, and hence the value of $\overline{\theta_v}$ is independent of height ($\overline{\theta_v}(z) = \text{const}$). As soon as cloud base is reached condensation occurs, and from that point $\theta_{v,u}$ follows a moist adiabatic profile, while the environment profile typically lies between that of a moist and a dry adiabat. This implies that above cloud base $\theta_{v,u}$ is increasing faster than $\overline{\theta_v}$, with the consequence that the farther above true cloud base the discrete cloud base is chosen, the larger the parcel excess in θ_v and hence T_v. By always choosing the model level above true cloud base as the discrete cloud-base level, as done in CTRL and CLEV, the parcel excess is necessarily larger than in all other experiments, as is evident in Fig. 4.

The final cloud-base property considered here is the cloud-base mass flux. Figure 5 shows the frequency distribution of this quantity. Note that in this figure the frequency of occurrence has been normalized with the total number of convective points. Hence, only relative changes at points that are convective can be deduced. It is evident that the average cloud-base mass flux in NCUB is significantly larger than in CTRL. Another obvious feature is a number of spikes at selected mass-flux values that become dramatically large with NCUB but are already present in CTRL. This leads to two questions. Why are the mass fluxes larger, and what leads to the observed peaks in the frequency distribution?

The first question can be answered by considering the closure for shallow convection [see Eq. (1)]. This closure is a typical example for an equilibrium closure, where it is assumed that the convective flux of moist static energy from the subcloud into the cloud layer is such that the mean subcloud moist static energy is conserved. It is obvious from (1) that the cloud-base mass flux directly depends on the parcel excess in moist static energy at cloud base. It can be inferred from Fig. 4 that this excess is significantly smaller in NCUB than in CTRL, leading to larger values of cloud-base mass flux.

The maxima in the frequency distribution at certain mass-flux values have been identified as a numerical artifact. The experiments performed here use the nominal time step for the T95L60 resolution, which is 1 h. With this relatively large time step and the high vertical resolution of the ECMWF model near the surface, the (explicit) solution of the mass-flux equations in the convection scheme can only remain stable if the local Courant–Friedrichs–Lewy (CFL) criterion is fulfilled. This criterion implies a maximum mass flux in a given layer that is defined as

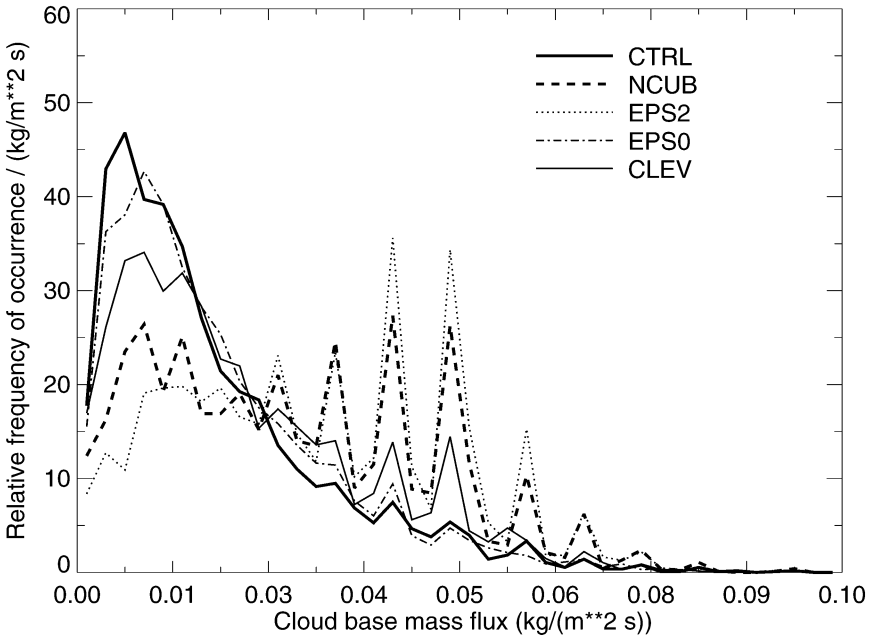

FIG. 5. Frequency distribution of cloud-base mass flux. Results are from the first time step of a T95L60 forecast and for the latitude band 30°N–30°S and are normalized by the total number of convective points for each experiment and unit mass flux.

$$M_b^{\max} = \frac{\Delta p}{g\Delta t}, \tag{8}$$

where Δp is the depth of the model layer, and Δt is the model time step. Assuming a surface pressure of 1013.25 hPa, the values for maximum mass flux for ECMWF model layers at typical cloud-base heights (200–600 m) are 0.027, 0.034, 0.042, 0.05, and 0.058 kg m^{-2} s^{-1}, respectively, well in-line with the location of the maxima in Fig. 5. This result clearly illustrates the increasing need for an implicit solver for the mass-flux scheme, as the CFL criterion is violated more often if models increase the time step and refine the vertical resolution.

The decision on the occurrence of convection in both algorithms is entirely based on subcloud layer properties and the fulfilment of some criteria at cloud base (a virtual temperature excess of more than −0.5 K in the current scheme or positive updraft vertical velocity in the new algorithm). In its current formulation, the next important decision that needs to be made in the ECMWF convection parameterization is the location of cloud top. This is so because the decision on convection type (shallow versus deep), which influences the choice of closure and entrainment rate, depends directly on cloud depth. In the CTRL model, cloud top is determined using an entirely thermodynamic criterion proposed by Arakawa and Schubert (1974), while NCUB uses a dynamical criterion based on finding at what height the updraft vertical velocity reverses sign (for details see section 2).

Figure 6 shows the cloud depth as determined by the CTRL and NCUB first-guess algorithms as well as the sensitivity in this case to the entrainment rate only (the sensitivity to w and CLEV is small). It is obvious that the two algorithms used in CTRL and NCUB give hugely different results. In CTRL many points are initially diagnosed to have convection deeper than 8 km, while in NCUB most of the points have cloud depths less than 2000 m. The sensitivity to entrainment rate is large, with higher (lower) entrainment rates yielding shallower (deeper) clouds. It is noteworthy that even the undilute version of NCUB diagnoses more shallow clouds than the original algorithm.

Given this result it is a legitimate question how the CTRL model provides the large number of shallow convective points seen in Fig. 2. The answer lies in the iterative nature of the scheme. After the first-guess calculation, which is the subject of this study, two iterations of a much more complex updraft calculation follow. It is obvious from Fig. 6 that the first-guess calculation performed in CTRL is very inconsistent with the later calculations. This is further emphasized in Fig. 7, which compares the first guess to the final cloud depth for both CTRL and NCUB. It is evident that, although far from perfect, the NCUB algorithm provides a first guess much more in-line with the final result of the convection parameterization.

4. The impact on the model climate

The previous section has established the direct impact of changes to the treatment of the subcloud layer and the first-guess parcel model in the ECMWF convection

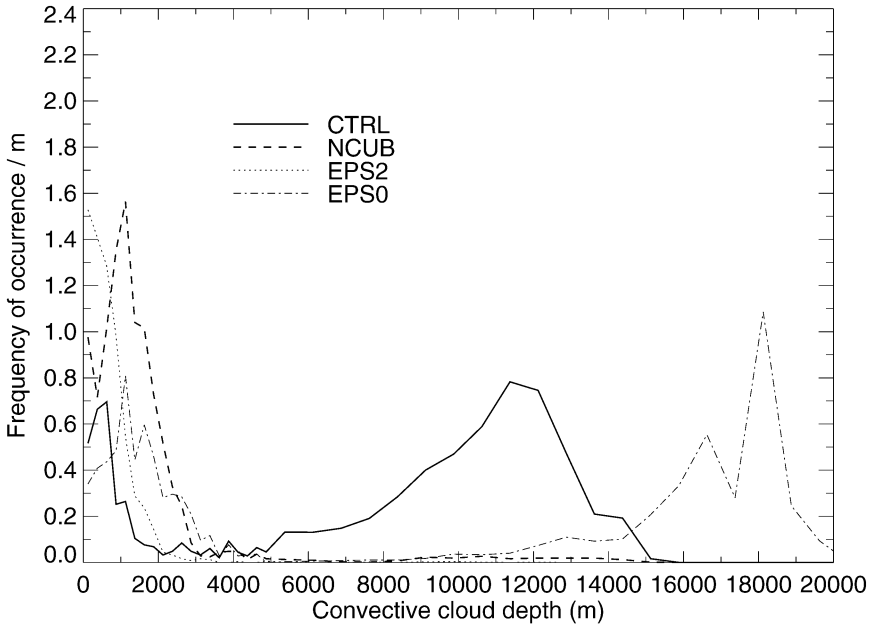

FIG. 6. Frequency distribution of convective cloud depth as given by the algorithms described in section 2. Results are from the first time step of a T95L60 forecast and for the latitude band 30°N–30°S. The frequency of occurrence has been normalized per unit depth to account for varying bin width due to varying model vertical resolution.

scheme, as well as to the decision tree involved. It is obvious that if the model is run for longer than one time step, feedbacks will either reinforce or dampen the impacts seen in the single–time step experiments. Furthermore, given the relatively large impacts seen in those experiments, it is valid to investigate the impact on the overall model climate that results from the changes made.

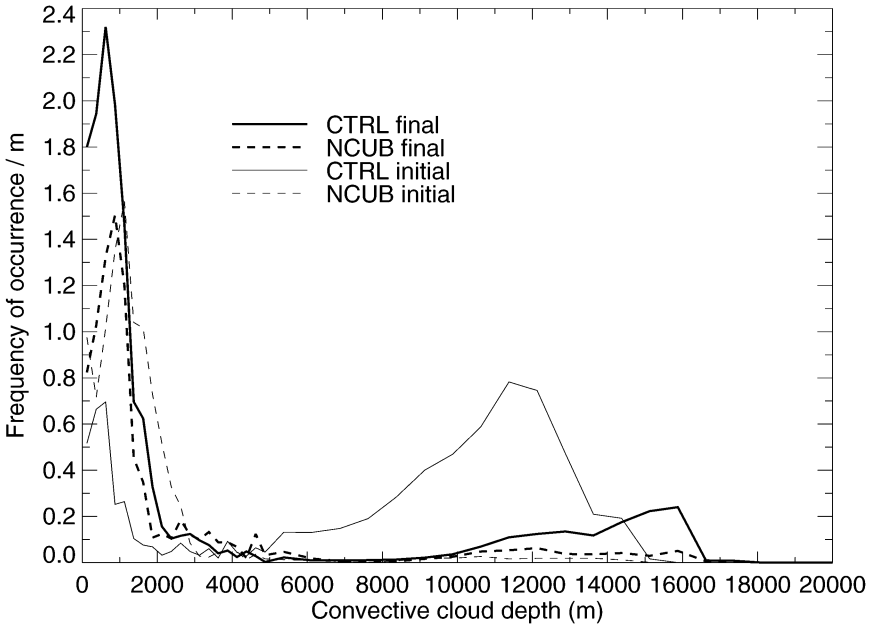

FIG. 7. Frequency distribution of convective cloud depth at the end of the full convection parameterization. Thin lines indicate the initial guess for cloud depth as shown in Fig. 6. Results are from the first time step of a T95L60 forecast and for the latitude band 30°N–30°S. The frequency of occurrence has been normalized per unit depth to account for varying bin width due to varying model vertical resolution.

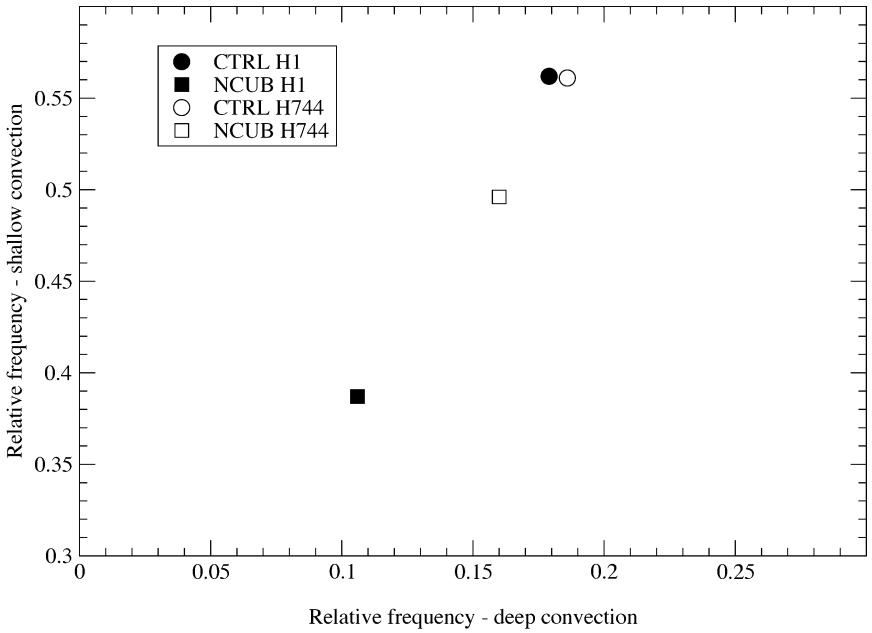

FIG. 8. Occurrence of surface-driven convection for CTRL and NCUB. Results are from the first time step and a time step after 744 h of integration of a T95L60 forecast and for the latitude band 30°N–30°S.

Figure 8 shows the occurrence statistics as in Fig. 2, but for a single time step after 744 h of integration in addition, and only for the CTRL and NCUB experiments. The occurrence of deep and shallow convection in the CTRL model is largely unaltered, with a minor increase in the number of deep convective events. The NCUB model, however, does show substantial increase in the occurrence of both convection types, in particular in that of shallow convection. This is indicative of feedback processes, which were deliberately excluded when looking at the first model time step only. Through these feedbacks, the thermodynamic state in the convective regions is slightly altered such that more convective points are established during the simulation. It is, however, worthwhile noting that even after 31 days of simulation NCUB produces significantly fewer convective points than CTRL.

The rest of this section will focus on changes in the overall model climate brought about by the NCUB algorithm. For this purpose, two ensembles of three 120-day integrations starting on 1, 2, and 3 November 1987, respectively, were carried out with the ECMWF model at T_L95 resolution with 60 model layers in the vertical. The first ensemble uses the CTRL scheme, while the second set is carried out with NCUB. The results are analyzed by forming ensemble and time averages for the months of December–January–February 1987/88 (DJF8788).

The examples chosen to illustrate the effect on the model climate are zonally averaged cloud cover (a), zonally averaged temperature (T), the zonally averaged zonal wind component, and global maps of precipitation. This set of variables does by no means constitute a comprehensive analysis of all possible changes. As highlighted in the introduction, it is the purpose of this paper to investigate the sensitivity of a GCM to supposedly basic assumptions made in one of its parameterization schemes. Therefore, the following figures serve illustrative purposes only.

Figure 9 shows the results for the zonally averaged cloud cover as a function of pressure for the tropical and subtropical latitudes. The CTRL model (top panel) exhibits cloud cover maxima in the upper tropical and lower troposphere. These maxima can be attributed to clouds generated by the model's deep and shallow convection schemes, which are strongly coupled to the model's cloud parameterization (Tiedtke 1993; Jakob 2001). The middle panel shows the results for the NCUB model, with the differences depicted in the lower panel. There are three noteworthy impacts of the new parameterization on the cloud fields:

1) The upper-tropospheric maximum in cloud cover is strongly reduced.
2) The lower-tropospheric maximum is enhanced.
3) A new maximum in cloud cover in the middle troposphere (around 600 hPa) is apparent.

Since most of the clouds in the Tropics are generated through convective processes, it should not be surprising that there is a change in cloud cover when the convection parameterization is altered. The magnitude of the change is, however, surprisingly large. Recent studies (e.g., Johnson et al. 1999) point out that the long-advocated picture of tropical convection producing a bi-

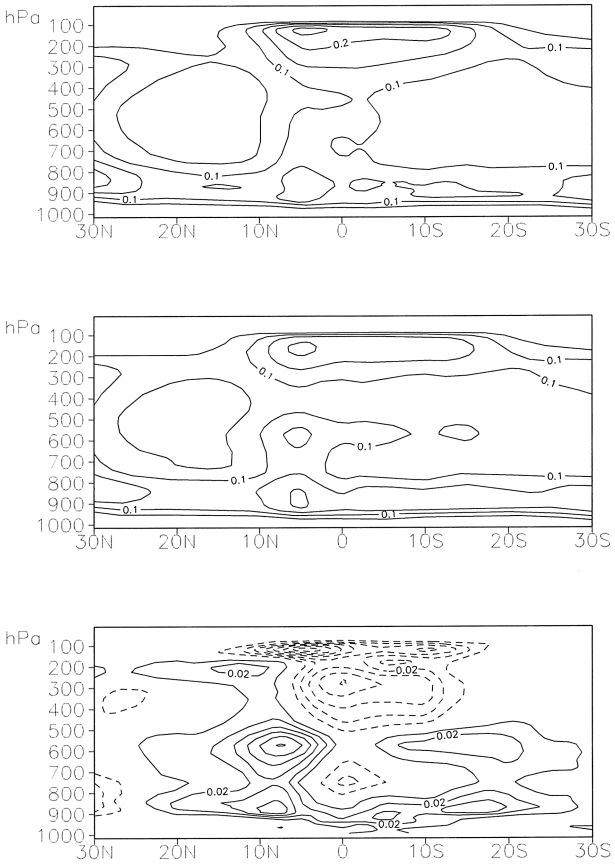

FIG. 9. Zonal mean cloud cover in (top) the CTRL model, (middle) the NCUB model, and (bottom) the difference NCUB-CTRL. The results are ensemble averages of a three-member ensemble of T95L60 integrations for DJF87/88, initialized on 1, 2, and 3 Nov 1987, respectively.

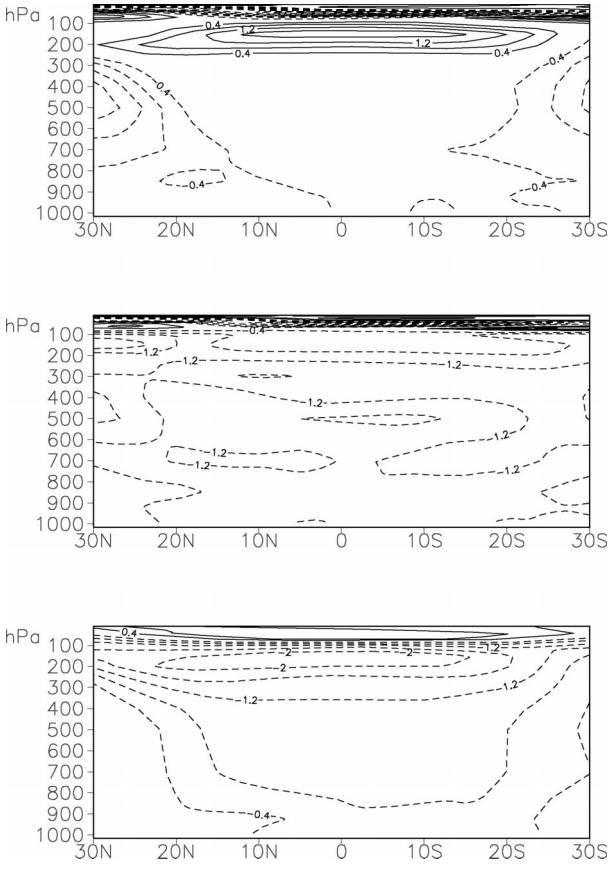

FIG. 10. Zonal mean temperature error in (top) the CTRL model, (middle) the NCUB model, and (bottom) the difference NCUB-CTRL. The results are ensemble averages of a three-member ensemble of T95L60 integrations for DJF87/88, initialized on 1, 2, and 3 Nov 1987, respectively. The error is calculated with respect to the ECMWF reanalysis.

modal distribution of convective cloud depth is unrealistic and that a third mode, with tops near the melting level, is often present in nature. In the light of these studies, one might be tempted to interpret the third peak in cloud cover near the location of the melting level as a model improvement, but in the absence of data it is difficult to judge whether the magnitude of the maximum is anywhere near realistic. The changes in cloud cover shown in Fig. 9 do, however, lead to some significant model responses outlined in the next two figures.

Figure 10 shows the zonally averaged temperature error with respect to the ECMWF reanalysis (ERA; Gibson et al. 1997) for the CTRL model (top) and the NCUB model (middle). The bottom panel shows the difference (NCUB − CTRL) between the two sets of simulations. The CTRL model exhibits a large positive temperature error between 300 and 100 hPa, peaking at values of more than 1.6 K at tropical latitudes and extending into the subtropics of both hemispheres. Overlying the tropospheric warm bias is a stratospheric cold bias of even greater magnitude. This dipole structure has been shown to be linked to the radiative effects of clouds (e.g., Slingo and Slingo 1988; Randall et al. 1989). It is therefore not surprising that the large change in upper tropospheric cloud cover, seen in Fig. 9, leads to a strong modification of the temperature biases in the NCUB model. As is apparent from the bottom panel, NCUB leads to a cooling throughout the troposphere, with a small warming in the lower stratosphere. As a consequence, the upper-tropospheric warm bias has been replaced by a (smaller in magnitude) cold bias. The middle and lower troposphere, which were almost bias free in CTRL, show a significant cold bias in NCUB.

One consequence of the large effect on temperature of the changes made in NCUB is a strong reduction of the (erroneously large) horizontal temperature gradient in the upper troposphere between tropical and extratropical latitudes. Through a simple consideration of the thermal wind balance, one would expect an effect of this change on the zonal wind field. This is demonstrated in Fig. 11, which shows the error (with respect to ERA) in the zonally averaged zonal wind for CTRL (top), NCUB (middle), and NCUB − CTRL (bottom). The

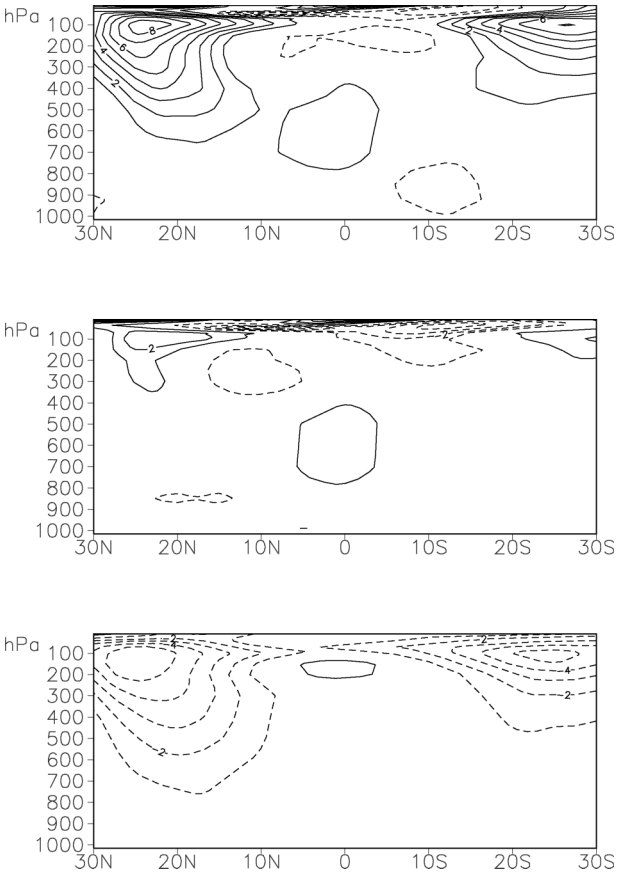

FIG. 11. Zonal mean error of zonal wind in (top) the CTRL model, (middle) the NCUB model, and (bottom) the difference NCUB-CTRL. The results are ensemble averages of a three-member ensemble of T95L60 integrations for DJF87/88, initialized on 1, 2, and 3 Nov 1987, respectively. The error is calculated with respect to the ECMWF reanalysis.

obvious reduction in zonal wind speed in NCUB constitutes a major improvement of the model error with respect to ERA.

Finally, Fig. 12 shows the effect of the changes on the mean model precipitation. Displayed are the DJF8788 ensemble average precipitation to the NCUB model (top), the difference between NCUB and CTRL (middle), and the difference in the convective component of the precipitation only (bottom). It is evident from the bottom panel that a major change in deep convective activity (as measured by convective precipitation) has occurred. There is a strong reduction in convective precipitation over most of the oceanic parts of the intertropical convergence zone (ITCZ), while precipitation over the tropical land areas is increased. An enhancement of total precipitation (middle panel) on the sides of the ITCZ indicates a broadening of the convergence zone in the model. An enhancement of precipitation in the South Pacific convergence zone (SPCZ) is also evident. It is difficult to assess whether these changes constitute a model improvement or not. The answer to this question depends on the dataset they are compared against, and is often inconclusive. The increase of rainfall over the tropical land areas, very likely connected to a difference in the simulated Walker circulation, appears to yield a more realistic model climate though.

5. Conclusions

This study has investigated the impact of a more sophisticated formulated parcel model used in the early decision-making processes of the ECMWF model's convection parameterization on the simulation of convection and its consequences for the model climate. It has been found that this supposedly small part of the parameterization problem has major consequences for both of these aspects of the model simulation.

The convection parameterization itself is affected in various ways:

- The occurrence of convection and in particular the types (shallow or deep) chosen are strongly altered.
- The change of cloud-base properties through the use of an entraining plume model leads to a substantial change in cloud-base mass flux and hence the strength of individual convective events.

The results of the work presented here are only valid strictly for the ECMWF model and may appear of little relevance to other parameterization schemes. However, several more general problems for the parameterization of convection have been exposed:

1) The sequence of using a ''first guess'' algorithm to define convective types and then perform a different set of calculations depending on the decisions made is undesirable. Its existence is a consequence of the nonunified approach to convection in bulk mass-flux parameterizations in general by assuming the existence of distinct convection types.
2) A number of problems in widely used closure assumptions have been demonstrated. Convection closures, such as the PBL equilibrium closure used here for shallow convection, often attempt to match fluxes of thermodynamic properties at cloud base. In the mass-flux approach, the fluxes are the product of the mass flux itself and an excess of the property in the convective drafts with respect to the environment. As shown in this study, the so-matched mass flux directly depends on the choice of the parcel model used in the updraft calculation. This can and will have consequences not only for the simulation of convection itself, but also for the simulation of convectively generated clouds if the now quite common approach of direct coupling clouds to the convective mass flux is used (e.g., Tiedtke 1993). It appears from this work that ''flux matching'' closures at cloud base are undesirable for mass-flux convection parameterizations.
3) Numerical choices are of crucial importance. This is

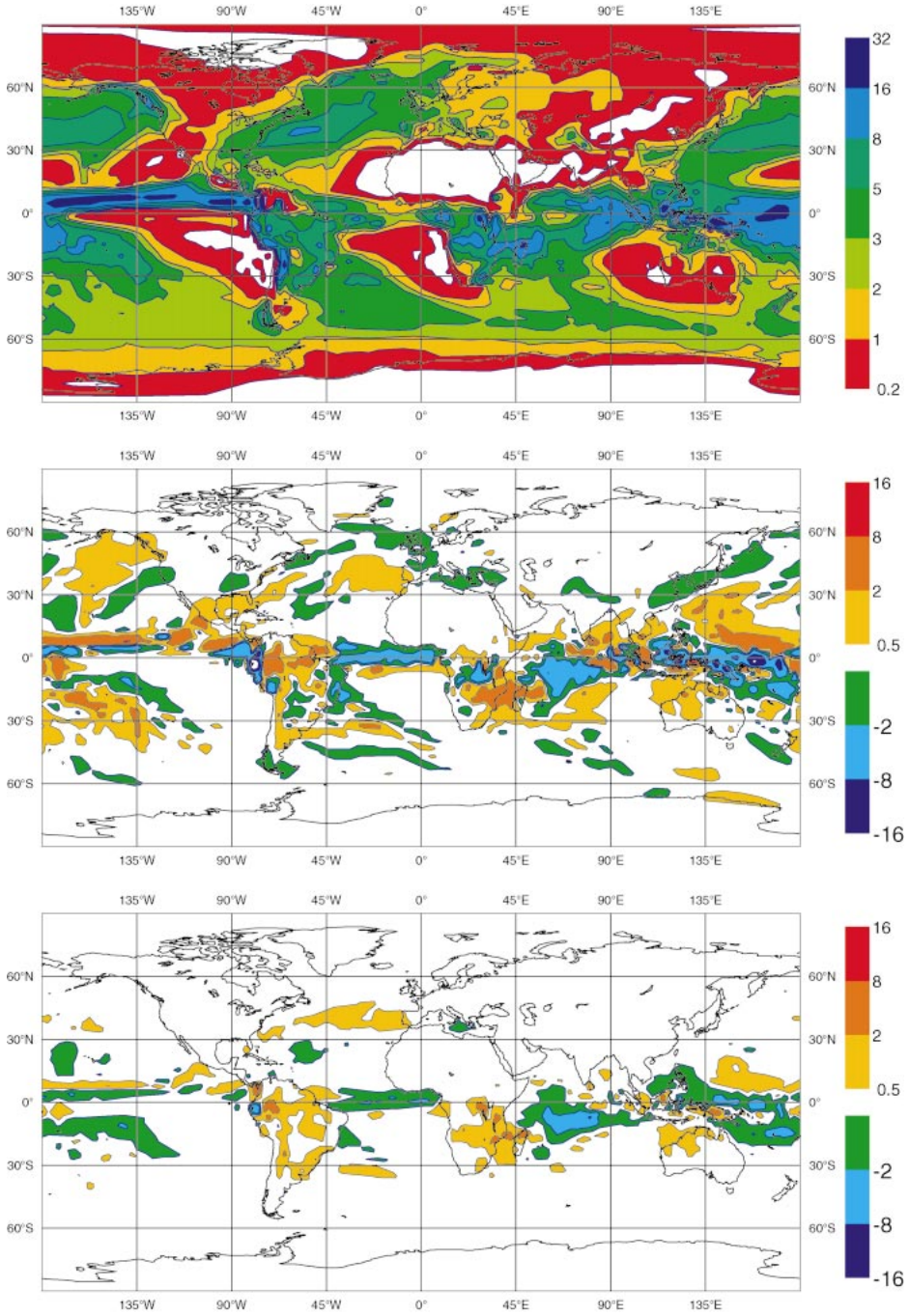

FIG. 12. (top) Mean precipitation for DJF87/88 for the NCUB experiment, (middle) the difference in total precipitation between NCUB and CTRL, and (bottom) the difference in convective precipitation between NCUB and CTRL. The results are ensemble averages of a three-member ensemble of T95L60 integrations for DJF87/88, initialized on 1, 2, and 3 Nov 1987, respectively.

exemplified here by the change in the choice of the discrete cloud-base level. As was shown, this ''simple'' choice directly affects the virtual temperature excess, with direct feedback on the closure. Furthermore, the large mass fluxes that are found because of smaller parcel excess (see previous item) lead to numerical problems in the solution of the advection part of the mass-flux solver.

The problems listed above are general problems that require attention in the various convection parameterizations used in GCMs. The most discomforting result

of this study, however, is that the model climate is strongly affected by the choices made. It needs to be pointed out again that the core of the ECMWF convection parameterization remained unaltered throughout this work. All that was changed were some of the first-guess decisions that are necessary in this type of parameterization. Since there will always be a certain degree of artificial choices (tuning), it appears prudent to reduce their importance. While there is no guarantee that a more unified approach to the convection parameterization problem will fully achieve this goal, it appears likely that a reduction in model sensitivities can be more easily achieved in such a framework. What we aim to demonstrate here is that a consistent treatment of the subcloud layer needs to be an integral part of any such approach.

Acknowledgments. We would like to thank Anton Beljaars, Martin Miller, and Martin Koehler at ECMWF for their support of this work and Aad van Ulden at KNMI for many useful discussions on the parcel formulation. Two anonymous reviewers helped to improve the quality of the manuscript. We also kindly acknowledge financial support from the EU-funded project EUROCS (Contract Number EVK2-CT-1999-00051).

REFERENCES

Arakawa, A., and W. H. Schubert, 1974: Interaction of a cumulus cloud ensemble with the large-scale environment, Part I. *J. Atmos. Sci.,* **31,** 674–701.

Betts, A. K., 1973: Non-precipitating cumulus convection and its parameterization. *Quart. J. Roy. Meteor. Soc.,* **99,** 178–196.

de Roode, S. R., P. G. Duynkerke, and A. P. Siebesma, 2000: Analogies between mass-flux and Reynolds-averaged equations. *J. Atmos. Sci.,* **57,** 1585–1598.

Donner, L. J., C. J. Seman, and R. S. Hemler, 2001: A cumulus parameterization including mass fluxes, convective vertical velocities, and mesoscale effects: Thermodynamic and hydrological aspects in a general circulation model. *J. Climate,* **14,** 3444–3463.

Emanuel, K. A., and M. Zivkovi-Rothman, 1999: Development and evaluation of a convection scheme for use in climate models. *J. Atmos. Sci.,* **56,** 1766–1782.

Fritsch, J. M., and C. F. Chappell, 1980: Numerical prediction of convectively driven mesoscale pressure systems. Part I: Convective parameterization. *J. Atmos. Sci.,* **37,** 1722–1733.

Gibson, J. K., P. Kållberg, S. Uppala, A. Hernandez, A. Nomura, and E. Serrano, 1997: ERA description. ECMWF Re-Analysis Project Report Series 1, 72 pp.

Grant, A. L. M., and A. R. Brown, 1999: A similarity hypothesis for shallow-cumulus transports. *Quart. J. Roy. Meteor. Soc.,* **125,** 1913–1936.

Gregory, D., 2001: Estimation of entrainment rate in simple models of convective clouds. *Quart. J. Roy. Meteor. Soc.,* **127,** 53–72.

——, and P. R. Rowntree, 1990: A mass flux convection scheme with representation of cloud ensemble characteristics and stability-dependent closure. *Mon. Wea. Rev.,* **118,** 1483–1506.

——, J.-J. Morcrette, C. Jakob, A. C. M. Beljaars, and T. Stockdale, 2000: Revision of convection, radiation and cloud schemes in the ECMWF Integrated Forecasting System. *Quart. J. Roy. Meteor. Soc.,* **126,** 1685–1710.

Hack, J. J., 1994: Parameterization of moist convection in the National Center for Atmospheric Research Community Climate Model (CCM2). *J. Geophys. Res.,* **99,** 5551–5568.

Holtslag, A. A. M., and C.-H. Moeng, 1991: Eddy diffusivity and countergradient transport in the convective atmospheric boundary layer. *J. Atmos. Sci.,* **48,** 1690–1698.

Hortal, M., 1999: The development and testing of a new two-time-level semi-Lagrangian scheme (SETTLS) in the ECMWF forecast model. ECMWF Tech. Memo. 292, 17 pp.

Jakob, C., 2001: The representation of cloud cover in atmospheric general circulation models. Ph.D. thesis, Ludwig-Maximilians-Universität München, 193 pp.

——, and S. A. Klein, 1999: The role of vertically varying cloud fraction in the parameterization of microphysical processes in the ECMWF model. *Quart. J. Roy. Meteor. Soc.,* **125,** 941–965.

——, and ——, 2000: A parametrization of the effects of cloud and precipitation overlap for use in general-circulation models. *Quart. J. Roy. Meteor. Soc.,* **126,** 2525–2544.

Johnson, R. H., T. M. Rickenbach, S. A. Rutledge, P. E. Ciesielski, and W. H. Schubert, 1999: Trimodal characteristics of tropical convection. *J. Climate,* **12,** 2397–2418.

Kain, J. S., and J. M. Fritsch, 1992: The role of the convective ''trigger function'' in numerical forecasts of mesoscale convective systems. *Meteor. Atmos. Phys.,* **49,** 93–106.

Neggers, R. A. J., A. P. Siebesma, and H. J. J. Jonker, 2002: A multiparcel model for shallow cumulus convection. *J. Atmos. Sci.,* **59,** 1655–1668.

Raga, G. B., J. B. Jensen, and M. B. Baker, 1990: Characteristics of cumulus band clouds off the coast of Hawaii. *J. Atmos. Sci.,* **47,** 338–355.

Randall, D. A., and D.-M. Pan, 1993: Implementation of the Arakawa–Schubert cumulus parameterization with a prognostic closure. *The Representation of Cumulus Convection in Numerical Models, Meteor. Monogr.,* No. 46, Amer. Meteor. Soc., 137–144.

——, Harshvardahan, D. A. Dazlich, and T. G. Corsetti, 1989: Interactions among radiation, convection and large-scale dynamics in a general circulation model. *J. Atmos. Sci.,* **46,** 1943–1970.

——, K.-M. Xu, R. J. Somerville, and S. Iacobellis, 1996: Single-column models and cloud ensemble models as links between observations and climate models. *J. Climate,* **9,** 1683–1697.

Raymond, D. J., and A. M. Blyth, 1986: A stochastic mixing model for nonprecipitating cumulus clouds. *J. Atmos. Sci.,* **43,** 2708–2718.

Siebesma, A. P., 1998: Shallow cumulus convection. *Buoyant Convection in Geophysical Flows,* E. J. Plate et al., Eds., Kluwer Academic, 441–486.

——, and J. W. M. Cuijpers, 1995: Evaluation of parametric assumptions for shallow cumulus convection. *J. Atmos. Sci.,* **52,** 650–666.

——, and J. Teixeira, 2000: An advection–diffusion scheme for the convective boundary layer: Description and 1D-results. Preprints, *14th Symp. on Boundary Layers and Turbulence,* Aspen, CO, Amer. Meteor. Soc., 133–136.

Simpson, J., and V. Wiggert, 1969: Models of precipitating cumulus towers. *Mon. Wea. Rev.,* **97,** 471–489.

Slingo, A., and J. M. Slingo, 1988: The response of a general circulation model to cloud longwave radiative forcing. I: Introduction and initial experiments. *Quart. J. Roy. Meteor. Soc.,* **114,** 1027–1062.

Tiedtke, M., 1989: A comprehensive mass flux scheme for cumulus parameterization in large-scale models. *Mon. Wea. Rev.,* **117,** 1779–1800.

——, 1993: Representation of clouds in large-scale models. *Mon. Wea. Rev.,* **121,** 3040–3061.

Troen, I., and L. Mahrt, 1986: A simple model of the atmospheric boundary layer: Sensitivity to surface evaporation. *Bound.-Layer Meteor.,* **37,** 129–148.

van Ulden, A. P., and A. P. Siebesma, 1997: A model for strong updrafts in the convective boundary layer. Preprints, *12th Symp. on Boundary Layers and Turbulence,* Vancouver, BC, Canada, Amer. Meteor. Soc., 257–259.

Zhang, G. J., and N. A. McFarlane, 1995: Sensitivity of climate simulations to the parameterization of cumulus convection in the Canadian Climate Centre General Circulation Model. *Atmos.–Ocean,* **33,** 407–446.